Quasistatic reduced yield stress number in London–van der Waals interacting solid-liquid media: Influence of high solid mass concentrations

Stefano A. Mezzasalma
Materials Science and Engineering Institute, University of Genoa, Corso Perrone 24A, 16161 Genova, Italy
(Received 11 April 1997; revised manuscript received 23 October 1997)

A set of ∞^1 functions, dependent on a parameter, is theoretically constructed to investigate the influence of the solid mass concentration c_n on the (quasi)static yield stress τ_0 of a liquid dispersion of solid particles near or at the isoelectric point and ruled by Derjaguin-Vervey-Landau-Overbeek interactions. The yield stress has been described as the force per unit area necessary to break two-particle clusters governed by attractive London–van der Waals interactions. As soon as an external stress begins to move the slurry, in the limit of zero velocity profile, the interparticle potential averaged over the cluster volume at the equilibrium state approaches the value deriving from the Hamaker law and gives rise to a relationship involving τ_0 and c_n. The achieved theoretical curves closely agree with experimental data concerning Si_3N_4, Zr_2O and $Ca_3(PO_4)_2$ aqueous suspensions as well as flocculated Al_2O_3 systems. Correspondingly, the parameter value turns out to be predictable from a phenomenological relationship involving the Hamaker constant and/or the mean interparticle energy. Theoretical descriptions were formulated in terms of a ''reduced yield stress number'' ($\zeta = \tau_0/\tilde{\tau}_0$, for some experimental value $\tilde{\tau}_0$), which accounts for the contribution associated to dispersion forces. [S1063-651X(98)00603-5]

PACS number(s): 83.50.−v, 82.70.−y

I. INTRODUCTION

The progress in understanding the static and dynamic yield stresses of (colloidal) suspensions of solid particles dispersed in a liquid medium is mainly due to the increased knowledge of interatomic-molecular and surface forces [1–15]. Thus, as the Derjaguin-Vervey-Landau-Overbeek (DLVO) theory [1,2,16,17] and its various modified formulations were suggested, many experimental and theoretical studies were able to state relations between dispersion rheology and electrochemistry, while, on the other hand, various conditions under which non-DLVO effects become notable (see, for instance, hydrophobic interactions among hydrocarbons) were obtained [1–8].

Briefly, the DLVO hypothesis consists of modeling the interparticle potential as a sum of two antagonistic terms: one repulsive, v_r, and the other attractive, v_a. The first, Coulombic, is related to the Debye-Huckel length of the diffused counterionic cloud in the slurry and to the double-layer electrostatic potential on the solid surface occurring by virtue of ionic adsorption-complexation phenomena from the liquid solution [1,2,18–21]; the second coincides with the weak dispersion force effects, essentially as Hamaker proposed in 1937 [11–13,22,23]. He reached the basic formulation of the London–van der Waals potential v_a for two spherical solid particles immersed in a medium; the formulation was improved in subsequent works by considering other specific contributions (geometry, etc.).

For two spherical aggregates A and B, of radii r_a and r_b and at a distance from the outest surfaces Δ_{ab}, such a relationship reads [22] $v_a = -[\mathcal{A} y_{ab}/12 x_{ab}(1+y_{ab})]$, where $\mathcal{A}(\simeq 10^{-(19\div 21)}$ J) is the Hamaker constant, characteristic of the A and B constituents, $y_{ab} = r_A/r_B$ and $x_{ab} = (\Delta_{ab}/2r_B)$ ($\ll 1$ in sufficiently concentrated suspensions). A first-attempt mean value is often written by setting $y_{ab} \simeq 1$ and $\overline{x} \simeq \overline{\Delta}/2r$ [2,16,17]:

$$\overline{v_a} \simeq -\frac{\mathcal{A}}{24\overline{x}^3}, \tag{1}$$

where $\overline{r}$ and $\overline{\Delta}$ are the average particle radius and the average interparticle distance from the outest surfaces [see Fig. 1(a)]. Equation (1) has been successfully employed in studying the

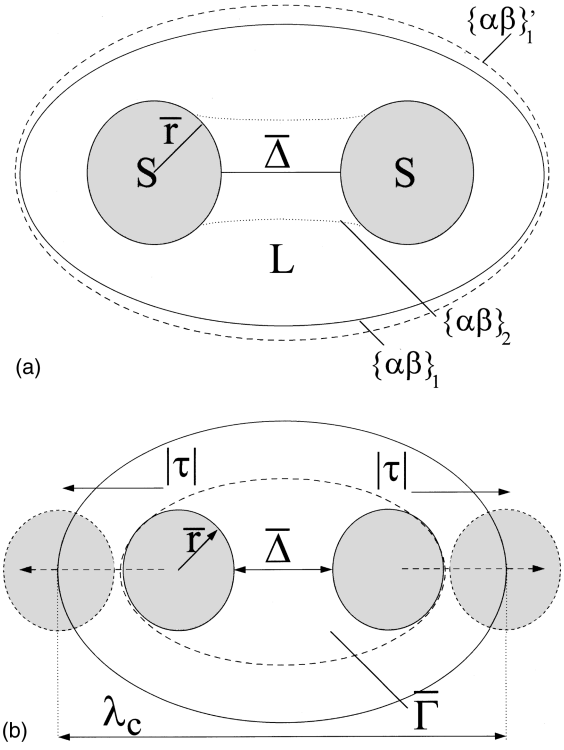

FIG. 1. Scheme of the equivalent two-particle cluster for a given geometrical configuration $\{\alpha,\beta\}$ (S, solid; L, liquid). (a) At the mechanical equilibrium. (b) At or near the yield point.

equilibrium of solid agglomeration phenomena in liquid dispersions of charged and/or one charged particles [1,17,24], or, more simply, of solid surfaces at separation distances that are not too small [1,23–25].

Accordingly, it is usually accepted that near or at the isoelectric point of a slurry [2,16,24] (iep or pH_{iep}), which stands for the zero surface charge point, the corresponding yield stress τ_0 is essentially ruled by attractive DLVO interactions, whose intensity increases with the solid mass concentration c_n [16,26–28]. Moreover, when non-DLVO effects are absent, the quasistatic yield stress τ decreases with the electrolyte concentration in the solution $c_\pm$ so that, in such cases, it is maximum at the iep [28–30], namely, $\tau_0 = \max_{c_\pm}\{\tau(c_\pm)\}$. In the presence of steric barriers due to the addition of flocculants, a modified DLVO attractive interaction can be improved by providing v_a to the adsorbate layer thickness onto the particle surface [2,16,17,24,26].

Therefore, to give a description of yield stress and related phenomena occurring in an interacting solid-liquid medium, it may be generally assumed that [16,24,31]

$$\langle|\tau|\rangle \propto |\langle -\nabla(v_a + v_r)\rangle|, \tag{2}$$

where the unknown proportionality constant (which in this notations is nonadimensional) takes into account hardly expressible phenomena, both macroscopic (such as finite size, shape effects, powder dispersibility [16,17,32], etc.) and microscopic (geometrical microstructure [33–35], chemistry [36,37], kinetics [38] and evolution of the solid-liquid surface tension [21,39], mixing entropy effects [7], etc.). First employments of Eq. (2) provided with phenomenological coefficients gave another successful confirmation of the validity of (modified and nonmodified) DLVO theories.

Unfortunately, the foregoing uncertainty is also influenced both by the adopted experimental method and by the physical model considered for interpreting τ theoretically. Indeed, a static yield stress can be expected when the general motion equation for the dynamic yield stress evolution [$\tau_\gamma = \tau_\gamma(t)$] includes a function $\mathcal{T}$ noninfinitesimal in the vanishing of the (angular) velocity (and/or frequency) $\dot\gamma$, i.e., $\lim_{\dot\gamma\to 0}\mathcal{T}\neq 0$ [40]:

$$\tau_\gamma(\eta,\dot\gamma,\tau,t) = T(\eta,\dot\gamma,\tau,t) + \mathcal{T}(\tau), \tag{3}$$

τ being the quasistatic yield stress, η the viscosity, and t the time, and where T is a general function representing the pure dynamic contribution, sometimes dependent on the system history, and such that $\lim_{\dot\gamma\to 0^+} T(\eta,\dot\gamma,\tau,t)=0$. Thus τ can generally be dependent on (a) the behavior of $\dot\gamma$ near zero [40,41], and on (b) the relation $\mathcal{T}=\mathcal{T}(\tau)$ that follows from the assumed rheological model (Bingham, Casson, etc.) [40].

Accordingly, in view of a quantitative description, yield stress ratios ($\zeta=\tau_0/\tilde\tau_0$, for an arbitrary measurement $\tilde\tau$), which will be called ''reduced yield stress numbers'' in the following, seem to be more significant than absolute values, implicitly supposing that the proportionality constants in Eq. (2) are equal in all experiments, and that non-DLVO effects do not occur [28]. Although to derive exact equations for τ and for all implied physicochemical quantities is a very tough task, the aforesaid methodology is certainly unsatisfactory, in particular, when strong electrostatic interparticle potentials arise and/or the complexity of aggregation processes increases [38,42]. Moreover, the knowledge of the phenomena is often restricted to information derived from best-fit functions only.

To give a first unified formulation, a family of curves based on classical DLVO assumptions is theoretically derived in this paper to describe the behaviors τ_0 vs c_n, even in the presence of steric barriers. All irreducible uncertainties are represented by an independent parameter (m) which, after a test conducted on several experimental data concerning Si_3N_4, ZrO_2, $Ca_3(PO_4)_2$ and Al_2O_3 liquid dispersions, turns out to be related to the Hamaker constant or, equivalently, to the value of the interaction energy among solid aggregates.

II. THEORETICAL DESCRIPTION

Statement of the problem. According to the literature, yield stress in a DLVO system will be regarded as the force per unit of dispersion area required to cause the cohesive strength exerted by London–van der Waals forces opposite to the arising of incipient motion [16,24,28–30] to vanish. Focusing yield stress behaviors as a function of the solid mass concentration near or at the iep, namely, τ_0 vs c_n, electrolyte effects [1,2,7,28,43] will not be attempted, nor electromagnetic fields [44] (see, for instance, electrorheological fluids [45]). Moreover, a population of equivalent two-particle systems will be dealt with as reflecting the global behavior of a dispersion at the given c_n and at the solid and liquid phase densities ρ_S and ρ_L [16,24].

The basic idea concerns two London-based interparticle potentials that, near or at the yield point of a solid-liquid system, approach the same value. In the first one, which is present before the beginning of the motion ($\dot\gamma=0$), two-particle clusters are considered in their equilibrium position. The second one, which is present at the beginning of the motion ($\dot\gamma\to 0^+$), refers to an equivalent cluster population that is moving from the initial configuration and that is subject to the original potential field. Accordingly, while at mechanical equilibrium the interparticle-intermolecular potential obeys the previous Hamaker equation (1) [22,23], when the slurry begins to move [see Fig. 1(b)] a mean interaction can be evaluated by averaging the foregoing relationship (1) near or at the incipient motion, namely, over the cluster volume where small displacements of solid agglomerates from their equilibrium positions can occur. For the sake of mathematical simplicity, a statistical approach written in the limit of zero velocity profile (i.e., which does not depend upon kinematics) will be developed in Sec. III, and, to this end, the dispersion energy will be geometrically averaged over the mean two-particle cluster volume that is evaluated near the equilibrium state.

Derivation of the set of functions $\{\tau_m(c_n)\}_m$. Consider a small (but finite) suspension volume Γ, where one pair of solid particles surrounded by a liquid medium is free to move [see Fig. 1(b)]. Let Γ be a generic volume enclosing both particles and suppose that $\Gamma\in(\Gamma_\mu,\overline{\Gamma})$ for some (limit) volume Γ_μ. If the probability dP_Γ to find the pair in $(\Gamma,\Gamma+d\Gamma)$ depends on a ν-power law of the form [46]

$$dP_\Gamma = \frac{d\Gamma^\nu}{|\overline{\Gamma}-\Gamma_\mu|^\nu}, \quad \nu\in\mathbb{R}, \tag{4}$$

the mean interaction is [47]

$$\hat{\bar{v}}_a=\frac{|\int_{\Gamma_\mu}^{\overline{\Gamma}} v_a d\Gamma^\nu|}{|\overline{\Gamma}-\Gamma_\mu|^\nu}, \tag{5}$$

that, by use of the Hamaker formula (1), becomes

$$\hat{\bar{v}}_a=-\left|\frac{\mathcal{A}}{24(\overline{\Gamma}-\Gamma_\mu)^\nu}\int_{\Gamma_\mu}^{\overline{\Gamma}} x_\Gamma d\Gamma^\nu\right|. \tag{6}$$

The quantity $x_\Gamma=r/2\Delta$, which in interacting media reflects the agglomeration state, must be regarded as a function of the volume that in turn relates particle radius and particle distance. Thus, to integrate Eq. (6), a relationship for the distance Δ depending on the volume Γ and on the radius r is required and, at first attempt, it can be set [48]

$$\Delta_{\alpha\beta}(\Gamma)=\alpha\Gamma^{1/3}-\beta r, \tag{7}$$

α and β standing for average numerical coefficients obtainable from geometrical arguments. A simple rearrangement of the integrand yields

$$\hat{\bar{v}}_a=-\left|\frac{\mathcal{A}}{12(\overline{\Gamma}-\Gamma_\mu)^\nu}\int_{\Delta_\mu}^{\overline{\Delta}}\frac{r}{\Delta_{\alpha\beta}}d\Gamma^\nu(\Delta)\right|, \tag{8}$$

where, according to the correspondence stated in Eq. (7), assigning a distance for any volume, one has $\overline{\Delta}=\Delta_{\alpha\beta}(\overline{\Gamma})$ and $\Delta_\mu=\Delta_{\alpha\beta}(\Gamma_\mu)$. To establish instead the integration limits in Eq. (8), some observations are needed.

First, when $\dot{\gamma}\to 0^+$, if the London–van der Waals energy in Eq. (8) approaches the equilibrium value, according to the notations in Eqs. (1) and (3) the yield stress point holds:

$$\hat{\bar{v}}_a\to\overline{v_a}\leftrightarrow\tau_\gamma\to\mathcal{T}(\tau_0). \tag{9}$$

Correspondingly, the equivalent two-particle cluster is broken up and the distance from the outermost surfaces can be setted to the value given by the average linear size of the cluster volume per pair of solid aggregates $\simeq\lambda_C^3$ [see Fig. 1(b)]. Such a condition reads as follows:

$$\Delta_\mu\to\lambda_C\leftrightarrow\tau_\gamma\to\mathcal{T}(\tau_0), \tag{10}$$

and points out the first integration limit of Eq. (8). Since the second limit is given by the mean separation distance in the original two-particle system $\overline{\Delta}$, integral (5) coherently takes into account the contribution due to displacements from the mechanical equilibrium to the yield point.

The main steps concerning the calculation of integral (8) and the development of condition (9) are reported in the Appendix for $\nu=1$. Briefly, by placing $r=\overline{r}\simeq$const in the equation for $\Delta_{\alpha\beta}$ and adopting the foregoing integration limits, it can be proved that condition (9) is equivalent to a polynomial implicit function

$$\mathcal{F}(t_\lambda,s_\xi)\equiv\sum_{i=0}^{3} p_{it}s_\xi^i=0, \tag{11}$$

where

$$p_{it}=p_{it}(t_\lambda^m),\quad t_\lambda=\frac{\lambda_C}{\overline{\Delta}},\quad s_\xi=\frac{\overline{x}}{\xi\alpha}, \tag{12}$$

and provided that $p_{3t}=2t_\lambda-\frac{3}{2}-\ln t_\lambda-(t_\lambda^2/2)$, $p_{2t}=2(1-t_\lambda+\ln t_\lambda)$, $p_{1t}=-\ln t_\lambda$, and $p_{0t}=\frac{1}{3}(1-t_\lambda^3)$. Basic macroscopical properties of a dispersion, that is, relative mass concentrations and density of both solid-liquid phases [43], are instead enclosed in ξ:

$$\xi^3=\frac{\pi}{3}\left(1+\frac{1}{2R}\right),\quad R=\frac{\rho_L}{\rho_S}\frac{c_n}{1-c_n}\ , \tag{13}$$

where R is derived from an application of the mass-volume balance to the binary system $V_S/V_L=R$, V_S and V_L being the solid phase volume and the liquid phase volume, respectively. In Eqs. (11) and (12), m is a parameter accounting for a more general relationship for the yield stress as a function of the separation distance between the solid surfaces [28,46]. Generally speaking, setting $\tau=\tau(\Delta^\mu)$ and, as here, $\mu\neq m$, a dependence of the form $m=m(\mu)$ is expected. In addition, m reflects the passage from two-particle clusters to many-particle systems which should be considered when the probability distribution in Eqs. (4) and (5) must be defined exactly. Due to such hardly expressible effects, the meaning of m in principle must be regarded as semiempirical.

Based on Eqs. (11)–(13), it is possible to achieve the behavior of the reduced yield stress number $\zeta_\tau\equiv\tau_0/\widetilde{\tau}_0$ versus c_n according to the implied macroscopical quantities, and corresponding to an arbitrary experimental point $(\widetilde{c}_n,\widetilde{\tau}_0)$. In fact, as in the present case yield stress is directly related to the force associated with the Hamaker potential field [see Eq. (2) and Refs. [22,28]], i.e., $\tau_0\propto-(\partial\overline{v_a}/\partial\overline{\Delta})=-\mathcal{A}\overline{r}/12\overline{\Delta^2}$, by combining the definitions of t_λ and s_ξ [see Eqs. (12)], one can introduce the functions $\tau_\xi=t_\lambda/s_\xi\xi$ and $\tau_\alpha=(2\alpha\lambda_C)^{-1}$ so that $\tau_\xi\tau_\alpha=\overline{r}/\overline{\Delta^2}$, and

$$\tau_0\propto\tau_\alpha\tau_\xi, \tag{14}$$

which represents the separation of τ_0 in geometrical-shape (τ_α) and geometrical-massive (τ_ξ) contributions. This means that $\tau_\alpha\simeq$const, provided the equivalent two-particle cluster is characterized by unchanging chemical composition and a constant liquid phase volume, and provided that the shape coefficient α does not strongly depend on c_n. Therefore, when only the solid concentration is varying, the effect of the mass distribution on the yield point of a suspension governed by dispersion forces can be followed by introducing a ''reduced'' yield stress number

$$\zeta_\tau=\frac{\tau_0}{\widetilde{\tau}_0}\equiv\frac{\tau_\xi}{\tau_{\widetilde{\xi}}}, \tag{15}$$

where $\widetilde{\tau}_0=r_0(\widetilde{c}_n)$ and $\tau_{\widetilde{\xi}}=\tau_\xi(\widetilde{c}_n)$ are, respectively, the (arbitrary) experimental and theoretical values [the latter $\tau_{\widetilde{\xi}}$ is a number deriving from Eq. (11)] corresponding to a given solid mass concentration $\widetilde{c}_n$ employed in the measurements.

To proceed, from the volume balance and the previous definition of R in Eq. (13) [43], one has

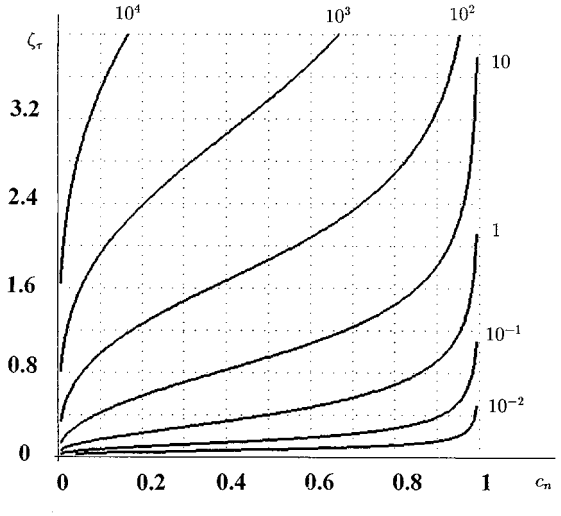

FIG. 2. Theoretical behaviors $\zeta_\tau=\zeta_\tau(c_n)$ for ρ_L/ρ_S less than or greater than 1 $(m=1)$. The numbers indicate the adopted density ratio values.

$$t_\lambda^3=\left(\frac{\lambda_C}{\overline{\Delta}}\right)^3\simeq\frac{\Sigma_i\,\dfrac{c_i}{\rho_i}}{\dfrac{1-c_n}{\rho_L}}=1+R, \tag{16}$$

or

$$c_n=-\frac{1}{1+\dfrac{\rho_L}{\rho_S t_\lambda^3}}, \tag{17}$$

which joins the ratio of the solid mass concentration to the density, and to the numerical solution of the theoretical model. Finally, from definitions (14) and (15), one obtains the relationship for the variable ζ_τ that is related to physical and numerical parameters in Eq. (17) through

$$\zeta_\tau=\frac{(t_\lambda^3-1)^{1/3}}{s_\xi}. \tag{18}$$

Once the solid and liquid density values are imposed, transformations (17) and (18), applied to the (t_λ,s_ξ) plane, describe the (c_n,ζ_τ) behavior parametrically in m. Equivalently, Eq. (11) gives a (t_λ,s_ξ) locus point which can be employed together with ρ_L and ρ_S to generate the fit function (c_n,ζ_τ) specified by applications (17) and (18) and dependent on a phenomenological coefficient. Before using the derived theoretical functions to interpret experimental data, it is worth noting that the ζ_τ behaviors shown in Fig. 2 for a fixed m value are monotonically increasing in c_n as well as in the density ratio ρ_L/ρ_S. Furthermore, in the limits of pure liquid and solid phases, one has, coherently,

$$\lim_{c_n\to 0}\zeta_\tau=0,\qquad \lim_{c_n\to 1}\zeta_\tau=+\infty, \tag{19}$$

while $\forall c_n=\tilde{c}_n<1$ no singularities occur. Based on three free parameters (ρ_L, ρ_S, and m), notice that the set of functions can coherently admit data collapses in correspondence of physically different solid-liquid systems.

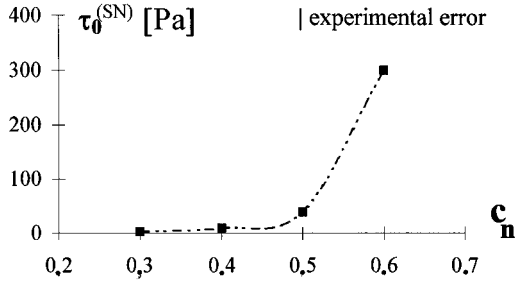

FIG. 3. Experimental behaviors $\tau_0^{(SN)}$ vs c_n of Si_3N_4/H_2O (1) suspensions at the iep (bar shows the experimental error).

III. EXPERIMENTAL DATA COMPARED WITH THEORETICAL PREDICTIONS

Experimental sections. Silicon nitride (SN) and tricalcium phosphate (TCP) nonporous powders were used as solid phases to prepare Si_3N_4 and Ca_3PO_4 aqueous suspensions at different solid mass concentrations. The physicochemical properties of the starting SN and TCP dried grains are described elsewhere [7]. The powders were dispersed in distilled water (pH=5.5) at room temperature ($T=293$ K) in a 250-ml beaker, and they were made homogeneous by placing the beaker in an ultrasound mixer for about 15 min. The slurries were then stirred in a strain-controlled universal rheometer and equilibrated for about 30 min before measurements. Isoelectric points of the slurries were obtained by using a metal-oxide-semiconductor ion-sensitive field-effect transistor pH meter [20,43,49], which made it possible to detect only the H^+ left in the liquid medium. They turned out to be $pH_{iep}^{(SN)}=8.0\pm0.1$ and $pH_{iep}^{(TCP)}=6.7\pm0.1$, respectively, for any solid mass concentration value.

Rheological measurements were made at room temperature and by using the Casson model which extrapolates for $\dot\gamma\to 0$ the static yield stress value according to the following relationship [7,40]:

$$\sqrt{\tau_\gamma}=\sqrt{\tilde\eta\dot\gamma}+\sqrt{\tau_0}, \tag{20}$$

$\tilde\eta$ being the viscosity of the dispersed system. As analyses of the motion equation (τ_γ) are not important here, extrapolated τ_0 values only will be reported and discussed in the following.

To obtain quasistatic yield stress values in the best experimental range of the rheometer, the applied velocity profiles were set to $\dot\gamma[s^{-1}]\leqslant 400$. In this range, the measurements were reproducible, and the relative experimental uncertainty turned out to be $|\delta\tau|/\tau\simeq(0.05/0.08)$. The achieved $\tau_0^{(SN)}$ and $\tau_0^{(TCP)}$ versus c_n behaviors are shown in Figs. 3 and 4.

Additionally, rheological data on zirconia (ZR) aqueous suspensions and on flocculated alumina (AL) systems dispersed in decalina will be examined together with the previous ones. Experimental details of the Zr_2O and Al_2O_3 systems are given elsewhere [27,28]. Here Figs. 5 and 6 illustrate the concerned measurements $\tau_0^{(ZR)}$ and $\tau_0^{(AL)}$ versus

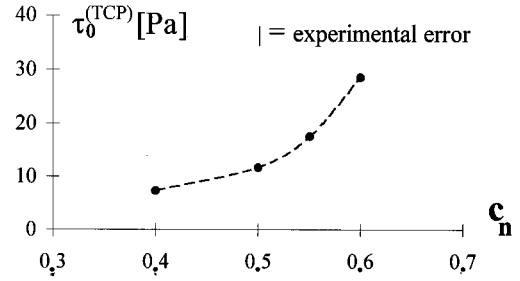

FIG. 4. Experimental behaviors $\tau_0^{(TCP)}$ vs c_n of $Ca_3(PO_4)_2/H_2O$ (1) suspensions at the iep (bar shows the experimental error).

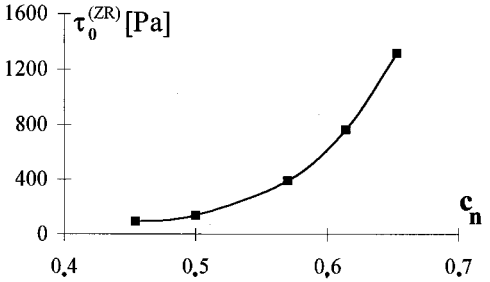

FIG. 6. Experimental measurements $\tau_0^{(ZR)}$ vs c_n of Zr_2O/H_2O (1) suspensions near or at the iep [28].

c_n. Recall that all quasistatic dispersion behavior investigated here at or near the iep are ruled by DLVO-based interactions.

Theoretical results and discussion. Experimental data were described by considering experimental reduced yield stress numbers, which consist of yield stress ratios normalized to the minimum of all $\tilde{\tau}_0$ measurements, i.e., $\zeta_\tau^{(i)} \geqslant 1 \forall \tilde{c}_n$ (i=SN,TCP,AL,ZR). As indicated in the end of the Sec. II, the locus point $s_\xi = s_\xi(t_\lambda)$ can be calculated numerically from Eq. (11) and, by using applications (17) and (18), the reduced yield stress number predicted by the model can be determined as a set of ∞^1 functions. A description of experimental $\zeta_\tau^{(i)}$ vs c_n behavior can be attempted according to the adopted m value. As Figs. 7–10 show, although the employed experimental methods were different, each set of measurements is well described by Eqs. (17) and (18) provided with an appropriate m value and the agreement between theory and experiments is quite satisfactory for all systems, including the flocculated modified DLVO dispersions.

Note that in the implicit function $s_\xi = s_\xi(t_\lambda)$ the entity of the interparticle energy is absent, whereas the yield stress certainly reflects the energetics of the suspension. Thus the only quantity related to the interaction strength is the phenomenological constant m [or, more rigorously, the value of ν in the probability function (4)]. If so, a relation linking m to the Hamaker constant $\mathcal{A}$ and/or the mean interparticle energy $\mathcal{E}$ would not be surprising. The m behavior shown in Fig. 11 indeed obeys the following relationship:

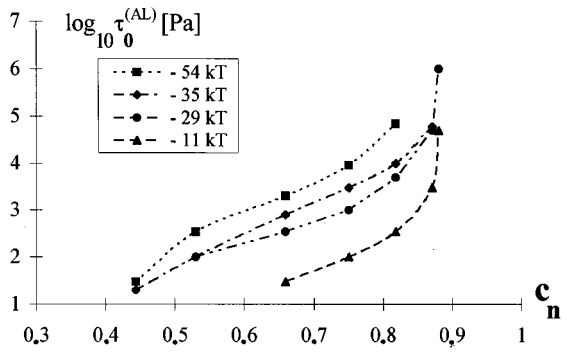

FIG. 5. Experimental measurements $\log_{10}\tau_0^{(AL)}$ vs c_n of Al_2O_3 suspensions dispersed in decalin for different values of the interparticle energy [27].

$$m(E_i) \propto \ln(cE_i), \quad E_i = \mathcal{A}_k, \mathcal{E}_r,$$
$$k = \text{TCP,SN,ZR}, \quad r = \text{AL,ZR}, \tag{21}$$

c being an empirical constant. All values of Hamaker constants are pointed out elsewhere [11,50–52], as well as the value of the interparticle energy among solid Zr_2O agglomerates dispersed in water [28].

It should be emphasized that Eq. (21) is only indicative. It simply states that the m value increases in the mutual attractive potential or, equivalently, in the long-range character of the concerned interaction. Nevertheless, due to the expected relation among the only phenomenological coefficient and the intrinsic intermolecular quantities and due to the close agreement between measured and predicted data, there are reasons for believing that further developments of the proposed method can increase the model predictability.

APPENDIX

Consider Eq. (8), provided with $\nu = 1$ and expressed as

$$\hat{\hat{v}}_a = -\left| \frac{\mathcal{A}}{12(\overline{\Gamma} - \Gamma_\mu)} \int_{\Gamma_\mu}^{\overline{\Gamma}} \frac{r}{\alpha\Gamma^{1/3} - \beta r}\, d\Gamma \right|, \tag{A1}$$

and assign to the two-particle cluster a geometrical configuration according to well defined α and β ranges and to a selected function of the form $r = r(\Gamma)$ [53]. Adopting $r \simeq \overline{r} = \text{const}$ to avoid overly difficult calculations, and recalling Eq. (7), integration of (A1) gives

$$\hat{\hat{v}}_a = -\frac{\mathcal{A}}{8\alpha^3(\overline{\Gamma} - \Gamma_\mu)} \left[\overline{\Delta}^2 - \Delta_\mu^2 + 4\beta\overline{r}(\overline{\Delta} - \Delta_\mu) + 2\beta^2\overline{r^2} \ln \frac{\overline{\Delta}}{\Delta_\mu} \right], \tag{A2}$$

from which, using conditions (9) and (10), one arrives at

$$\tfrac{2}{3}\alpha(\overline{\Gamma} - \lambda_C^3) = \overline{\Delta}^3 - \overline{\Delta}\lambda_C^2 + 4\beta\overline{\Delta}\overline{r}(\overline{\Delta} - \lambda_C) + 2\beta^2\overline{\Delta}\overline{r^2} \ln \frac{\overline{\Delta}}{\lambda_C}. \tag{A3}$$

Recalling that the mass balance for a binary system consisting of solid and liquid phase volumes V_S and V_L reads $V_S/V_L = R = (\rho_L/\rho_S)[c_n/(1-c_n)]$, once $\rho_{S,L}$ are known,

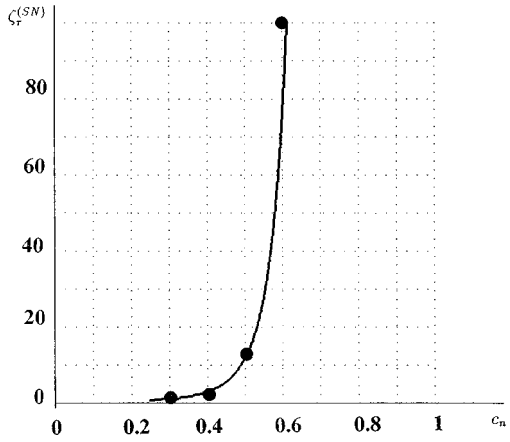

FIG. 7. Theoretical yield stress ratio $\zeta_\tau^{(\mathrm{SN})}=\zeta_\tau^{(\mathrm{SN})}(c_n)$ compared with experimental data derived from Fig. 3.

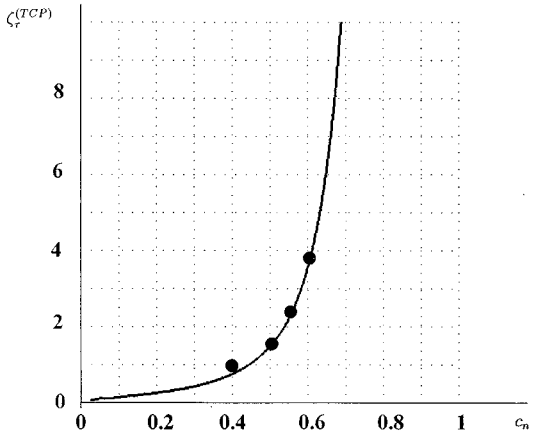

FIG. 8. Theoretical yield stress ratio $\zeta_\tau^{(\mathrm{TCP})}=\zeta_\tau^{(\mathrm{TCP})}(c_n)$ compared with experimental data derived from Fig. 4.

Eq. (A3) allows us to obtain one geometrical quantity only (i.e., Δ) as a function of the solid mass concentration, provided the other variable (i.e., $\overline{r}$) has already been determined. The last relationship can nevertheless be rearranged in a more suitable form. For spherical agglomerates, i.e., $\overline{v}\sim\frac{4}{3}\pi\overline{r}^3$ [and see Figs. 1(a) and 1(b)], development of the volume balance yields $\overline{\Gamma}=2\overline{v}\,[1+(1/2R)]$, or [43]

$$\overline{\Gamma}^{1/3}=2\xi\overline{r}, \tag{A4}$$

where $\xi=((\pi/3)[1+(1/2R)])^{1/3}$ was introduced in Eq. (13). Accordingly, using the definition of $\overline{x}\equiv\overline{\Delta}/2\overline{r}$ and combining Eq. (A4) with the geometrical constraint (7) for $\Delta_{\alpha\beta}$, it is possible to set

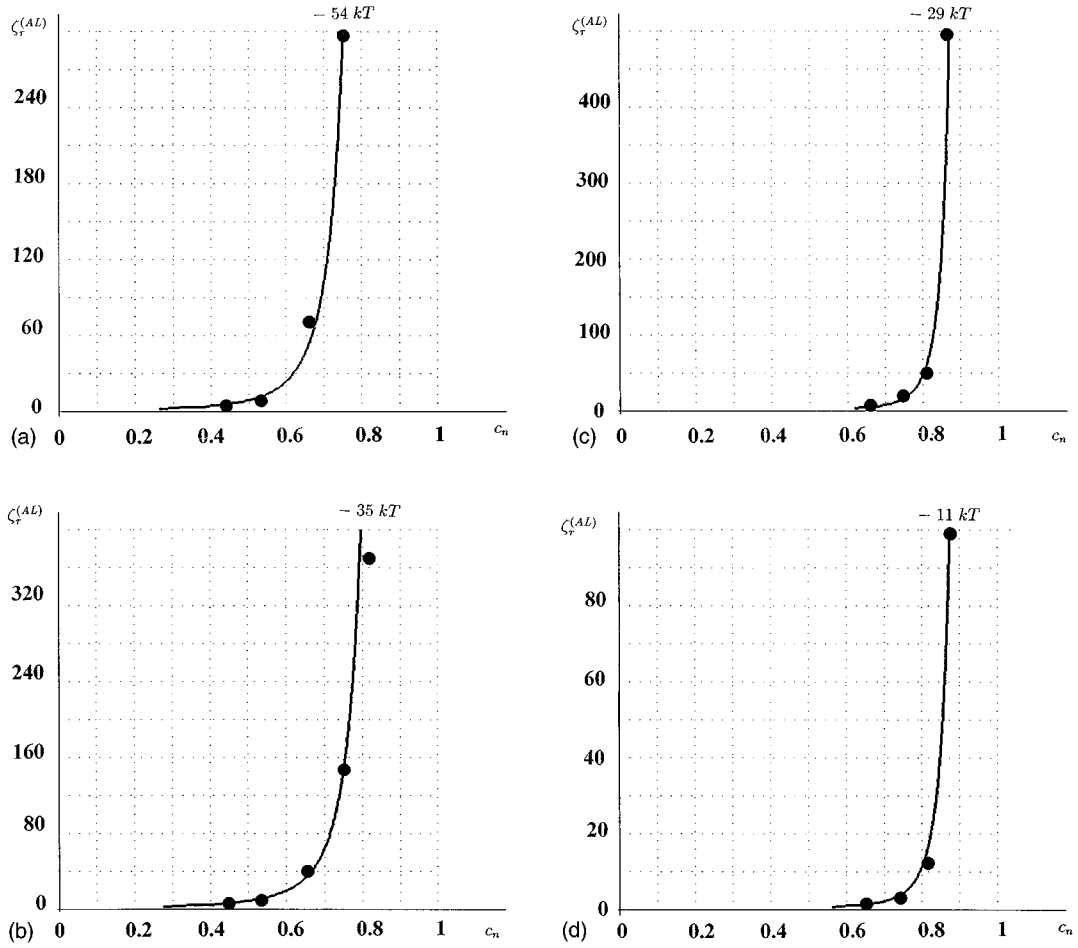

FIG. 9. (a)–(d) Theoretical yield stress ratio $\zeta_\tau^{(\mathrm{AL})}=\zeta_\tau^{(\mathrm{AL})}(c_n)$ compared with experimental data derived from Fig. 5.

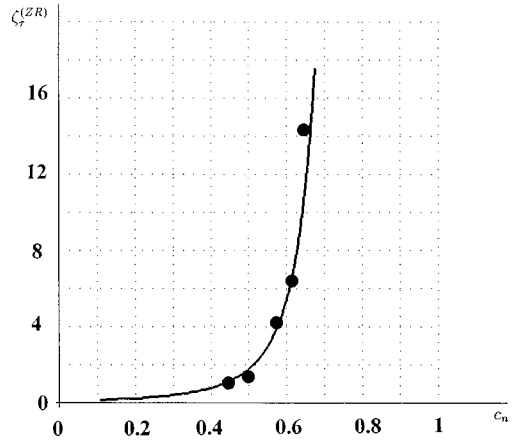

FIG. 10. Theoretical yield stress ratio $\zeta_\tau^{(\mathrm{ZR})}=\zeta_\tau^{(\mathrm{ZR})}(c_n)$ compared with experimental data derived from Fig. 6.

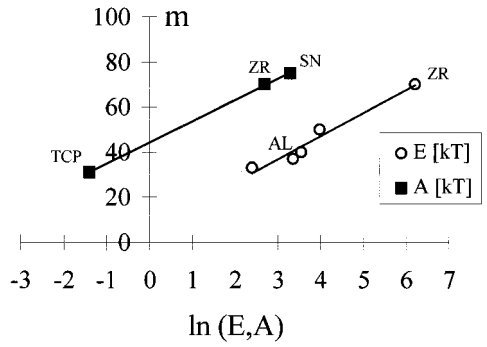

FIG. 11. Heuristic m coefficient as a function of the Hamaker constant $\mathcal{A}[kT]$ and of the interaction energy $\varepsilon\,[kT]$.

$$\frac{\beta}{2}=\xi\alpha-\overline{x.} \tag{A5}$$

Substitution of Eqs. (A4) and (A5) into Eq. (A3), and some algebraical manipulations, then lead to

$$\left(\ln\frac{\overline{x}}{x_\lambda}-\frac{3}{2}\right)\overline{x^2}+2\overline{x}\left[\xi\alpha\left(1-\ln\frac{\overline{x}}{x_\lambda}\right)+\overline{x_\lambda}\right]$$

$$+\xi\alpha\left(\xi\alpha\,\ln\frac{\overline{x}}{x_\lambda}-2\overline{x_\lambda}\right)=\frac{(\xi\alpha)^3}{3\overline{x}}, \tag{A6}$$

where $\overline{x/x_\lambda}\equiv\overline{\Delta}/\lambda_C$. Defining the quantities $s_\xi=\overline{x/}\xi\alpha$ and $t_\lambda=\overline{x_\lambda}/\overline{x}$, and dividing both members by $\overline{x^2}$, Eq. (A6) is transformed into a three-degree s_ξ polynomial:

$$p_{3t}s_\xi^3+p_{2t}s_\xi^2+p_{1t}s_\xi+p_{0t}=0, \tag{A7}$$

where $p_{3t}=2t_\lambda-\frac{3}{2}-\ln t_\lambda-(t_\lambda^2/2)$, $p_{2t}=2(1-t_\lambda+\ln t_\lambda)$, $p_{1t}=-\ln t_\lambda$, and $p_{0t}=\frac{1}{3}(1-t_\lambda^3)$.

Equation (A7) was derived by employing $\nu=1$ in the infinitesimal probability distribution (4). More generally, it is reasonable to expect that the ν coefficient in Eq. (4) will change with the specific solid plus liquid system. Thus, since its value is *a priori* unknown, a discussion of $\hat{\bar{v}}_a=\hat{\bar{v}}_a(\nu)$ may be required. The evaluation of integral (8) for a generic $\nu\in\mathbb{R}$ leads, however, to a quite complicated development of the solution as a power sum of the geometrical variables [54,55]. Generally, as already suggested elsewhere in different semiempirical approaches [28,46], it is more direct and effective to take into account the heuristic relationship $\tau=\tau(\Delta^m)$, and to insert the coefficient m in Eq. (A7) according to the global phenomenological position

$$t_\lambda\to t_\lambda^m\Rightarrow\sum_{i=0}^{3}p_i(t_\lambda^m)s_\xi^i,\quad m\in\mathbb{R}. \tag{A8}$$

If one combines Eq. (A8) and the implicit function (A7), the set of ∞^1 locus points $s_\xi=s_\xi(t_\lambda,m)$ follows.

Introducing the function $\tau_\xi=\tau_\xi(t_\lambda,s_\xi)$ in Eq. (14), the solid mass concentration c_n can be related to the reduced yield stress number ζ_τ according to Eqs. (14)–(16) and (A8). Results obtained in Eqs. (17) and (18) can be summarized as

$$\zeta_\tau(c_n)\equiv\{(c_n=1/[1+\rho_L/(\rho_S t_\lambda^3)],$$

$$\zeta_\tau=(t_\lambda^3-1)^{1/3}/s_\xi)\,|\,\mathcal{F}(t_\lambda,s_\xi)=0\}, \tag{A9}$$

from which the behavior $\zeta_\tau=\zeta_\tau(c_n)$ can be achieved when the density ratio ρ_L/ρ_S and the heuristic coefficient m are kept at constant values.

Finally, it should be noted that if strong electrostatic interactions act between particles, from previous works [7,20,21,39,42,43] concerning the influence of ionic adsorption-complexation phenomena on the particle size, it follows that the assumption of a constant radius within the cluster volume could fail. Therefore, far from the isoelectric point of the slurry, integrals (8) and (A1) becomes much more difficult to solve exactly.

ACKNOWLEDGMENTS

The author wishes to thank Professor D. T. Beruto and Professor P. M. Capurro for helpful discussions, and Dr. D. Baldovino and Dr. L. Risso for valuable assistance. This work was partially supported by the Italian Ministry of University and Research in Science and Technology.

[1] J. N. Israelachvili, *Intermolecular and Surface Forces* (Academic, London, 1985).
[2] E. Matijevic, *Surface and Colloid Science* (Plenum, New York, 1978).
[3] S. Marcelja, Chem. Phys. Lett. **42**, 129 (1976).
[4] R. M. Pashley, J. Colloid Interface Sci. **83**, 531 (1981).
[5] W. A. Ducker, Z. Xu, D. R. Clarke, and J. N. Israelachvili, J. Am. Ceram. Soc. **77**, 437 (1994).
[6] R. M. Pashley, P. M. McGuiggan, B. W. Ninham, and D. F. Evans, Science **229**, 1088 (1985).
[7] S. A. Mezzasalma, J. Colloid Interface Sci. **190**, 302 (1997).
[8] A. A. Kornyshev, D. A. Kossakowski, and S. Leikin, J. Phys. Chem. **97**, 6809 (1992).
[9] L. Guldbrand, B. Jonsson, H. Wennerstrom, and P. Linse, J. Chem. Phys. **80**, 2221 (1984).
[10] H. K. Christenson, P. M. Claesson, and J. L. Parker, J. Phys. Chem. **96**, 6725 (1992).
[11] J. Visser, Adv. Colloid Interface Sci. **3**, 331 (1972).
[12] J. Gregory, Adv. Colloid Interface Sci. **2**, 396 (1970).
[13] J. Lyklema, Adv. Colloid Interface Sci. **2**, 114 (1968).
[14] B. V. Derjaguin, S. S. Dukhin, and V. N. Shilov, Adv. Colloid Interface Sci. **13**, 141 (1980).
[15] S. S. Dukhin and V. N. Shilov, Adv. Colloid Interface Sci. **13**, 153 (1980).
[16] G. D. Parfitt, *Dispersion of Powders in Liquids* (Elsevier, London, 1969).
[17] R. D. Nelson, *Dispersion Powders in Liquids-Handbook of Powder Technology 7* (Elsevier, Amsterdam, 1988).
[18] J. O'M Bockris and A. K. N. Reddy, *Modern Electrochemistry* (Plenum-Rosetta, New York, 1970).
[19] G. D. Parfitt and C. H. Rochester, *Adsorption from Aqueous Solution at the Solid-Liquid Interface* (Academic, New York, 1983).
[20] S. Mezzasalma and D. Baldovino, J. Colloid Interface Sci. **180**, 413 (1996).
[21] D. Beruto, S. Mezzasalma, and P. Oliva, J. Colloid Interface Sci. **186**, 318 (1997).
[22] H. C. Hamaker, Physica IV **10**, 1058 (1937).
[23] J. N. Israelachvili, Contemp. Phys. **15**, 159 (1974).
[24] C. Galassi, *Chimica dei Colloidi e Reologia Applicata ai Ceramici* (CNR-IRTEC, Imola, 1992).
[25] M. L. Gee, P. Tong, J. N. Israelachvili, and T. A. Witten, J. Chem. Soc. Faraday Trans. **93**, 6057 (1990).
[26] L. Bergstrom, C. H. Schilling, and I. Aksay, J. Am. Ceram. Soc. **75**, 3305 (1992).
[27] L. Bergstrom, C. H. Schilling, and I. Aksay, J. Am. Ceram. Soc. **78**, 3225 (1995).
[28] Y. K. Leong, P. J. Scales, T. W. Healy, and D. V. Boger, J. Chem. Soc. Faraday Trans. **89**, 2473 (1993).
[29] R. J. Hunter and S. K. Nicol, J. Colloid Interface Sci. **28**, 250 (1968).
[30] Y. K. Leong, P. V. Liddell, T. W. Healy, and D. V. Boger (unpublished).
[31] J. C. Chang, F. F. Lange, and D. S. Pearson, J. Am. Ceram. Soc. **77**, 26 (1994).
[32] F. W. Wiegel and A. S. Perelson, J. Stat. Phys. **23**, 241 (1980).
[33] R. M. German, *Particle Packing Characteristics* (Metal Powders Industry Federation, New York, 1988).
[34] R. Mosseri and J.-F. Sadoc, *Geometry in Condensed Matter Physics* (World Scientific, Singapore, 1990).
[35] D. Weare and M. A. Fortes, Adv. Phys. **43**, 685 (1994).
[36] B. V. Velamakanni, F. F. Lange, F. W. Zok, and D. S. Pearson, J. Am. Ceram. Soc. **77**, 216 (1994).
[37] Y. K. Leong, D. V. Boger, and D. Parris, J. Rheol. **35**, 149 (1991).
[38] F. Family and D. P. Landau, *Kinetics of Aggregation and Gelations* (Elsevier, Amsterdam, 1984).
[39] S. A. Mezzasalma and R. Novakovic, J. Colloid Interface Sci. **190**, 294 (1997).
[40] R. B. Bird, W. E. Stewart, and E. N. Lightfoot, *Fenomeni di Trasporto* (Casa Editrice Ambrosiana, Milan, 1970).
[41] P. Doremus and J. M. Piau, J. Non-Newtonian Fluid Mech. **39**, 335 (1991).
[42] S. A. Mezzasalma, Phys. Rev. E **55**, 7137 (1997); see also S. A. Mezzasalma, Chem. Phys. Lett. **274**, 213 (1997); J. Chem. Phys. **107**, 9214 (1997).
[43] D. Beruto, S. Mezzasalma, and D. Baldovino, J. Chem. Soc. Faraday Trans. **91**, 323 (1995).
[44] G. Bossis and E. Lemaire, J. Rheol. **35**, 1345 (1991).
[45] R. T. Bonnecaze and J. F. Brady, J. Rheol. **36**, 73 (1992).
[46] D. H. Everett, *Colloid Science* (Chemical Society, London, 1973).
[47] F. Reif, *Fundamentals of Statistical and Thermal Physics* (McGraw-Hill, New York, 1965).
[48] P. Oliva (private communication).
[49] J. Janata, and R. J. Huber, *Solid State Chemical Sensors* (Academic Press, London, 1995).
[50] W.-H. Shih, D. Kisailus, and W. Y. Shih, J. Am. Ceram. Soc. **79**, 1155 (1996).
[51] J. C. Elliott, *Structure and Chemistry of the Apatites and Other Calcium Ortophosphate* (Elsevier, Amsterdam, 1994).
[52] R. C. Weast, *Handbook of Chemistry and Physics* (CRC, Cleveland, 1976).
[53] P. Oliva (personal communication).
[54] M. Fagiel, in *Handbook of Mathematical, Scientific and Engineering Formula, Tables, Functions, Graphs and Transforms* (Research and Education Association, New York, 1986).
[55] V. I. Smirnov, in *Corso di Matematica Superiore* (Riuniti, Rome, 1973).